ISSN 1674-1056
http://cpb.iphy.ac.cn
http://iopscience.iop.org/cpb
中国物理 B
Chinese Physics
中国物理 Chinese Physics B

16-channel dual-tuning wavelength division multiplexer/demultiplexer

Pei Yuan(袁配), Yue Wang(王玥), Yuan-Da Wu(吴远大), Jun-Ming An(安俊明), Xiong-Wei Hu(胡雄伟)

Citation: Chin. Phys. B . 2018, 27(12): 124208. **doi:** 10.1088/1674-1056/27/12/124208
Journal homepage: http://cpb.iphy.ac.cn; http://iopscience.iop.org/cpb

What follows is a list of articles you may be interested in

Geometrical representation of coherent tunneling process in two-waveguide and three-waveguide coupler

Jian Shi(时坚), Rui-Qiong Ma(马瑞琼), Zuo-Liang Duan(段作梁), Meng Liang(梁猛), Bao-Yu Chai(柴宝玉), Jun Dong(董军)
Chin. Phys. B . 2017, 26(12): 124214. **doi:** 10.1088/1674-1056/26/12/124214

Low power consumption 4-channel variable optical attenuator array based on planar lightwave circuit technique

Mei-Zhen Ren(任梅珍), Jia-Shun Zhang(张家顺), Jun-Ming An(安俊明), Yue Wang(王玥), Liang-Liang Wang(王亮亮), Jian-Guang Li(李建光), Yuan-Da Wu(吴远大), XiaoJie Yin(尹小杰), Xiong-Wei Hu(胡雄伟)
Chin. Phys. B . 2017, 26(7): 074221. **doi:** 10.1088/1674-1056/26/7/074221

High-efficiency focusing grating coupler with optimized ultra-short taper

Yang Biao, Li Zhi-Yong, Yu Yu-De, Yu Jin-Zhong
Chin. Phys. B . 2014, 23(11): 114206. **doi:** 10.1088/1674-1056/23/11/114206

Novel wavelength-accurate InP-based arrayed waveguide grating

Pan Pan, An Jun-Ming, Wang Hong-Jie, Wang Yue, Zhang Jia-Shun, Wang Liang-Liang, Dai Hong-Qing, Zhang Xiao-Guang, Wu Yuan-Da, Hu Xiong-Wei
Chin. Phys. B . 2014, 23(4): 044210. **doi:** 10.1088/1674-1056/23/4/044210

A high figure of merit localized surface plasmon sensor based on a gold nanograting on the top of a gold planar film

Zhang Zu-Yin, Wang Li-Na, Hu Hai-Feng, Li Kang-Wen, Ma Xun-Peng, Song Guo-Feng
Chin. Phys. B . 2013, 22(10): 104213. **doi:** 10.1088/1674-1056/22/10/104213

16-channel dual-tuning wavelength division multiplexer/demultiplexer*

Pei Yuan(袁配)[1,2], Yue Wang(王玥)[1,†], Yuan-Da Wu(吴远大)[1,2,‡], Jun-Ming An(安俊明)[1,2], and Xiong-Wei Hu(胡雄伟)[1]

[1] *State Key Laboratory on Integrated Optoelectronics, Institute of Semiconductors, Chinese Academy of Sciences, Beijing* 100083, *China*
[2] *College of Materials Science and Opto-Electronic Technology, University of Chinese Academy of Sciences, Beijing* 100083, *China*

(Received 27 June 2018; revised manuscript received 28 August 2018; published online 10 November 2018)

A 16-channel dual tuning wavelength division multiplexer/demultiplexer based on silicon on insulator platform is demonstrated, which is both peak wavelength tunable and output optical power tunable. The wavelength division multiplexer/demultiplexer consists of an arrayed waveguide grating for wavelength division multiplexing/demultiplexing, a heater for peak wavelength tuning and a variable optical attenuator based on p–i–n carrier-injection structure for optical power tuning. The experimental results show that the insertion loss on chip of the device is 3.7 dB–5.7 dB and the crosstalk is 7.5 dB–9 dB. For the tunability of the peak wavelength, 1.058-nm wavelength tunability is achieved with 271.2-mW power consumption, and the average modulation efficiency is 3.9244 nm/W; for the tunability of the optical power, the optical power equalization is achieved in all 16 channels, 20-dB attenuation is achieved with 144.07-mW power consumption, and the raise/fall time of VOA is 35 ns/42 ns.

Keywords: arrayed waveguide grating, variable optical attenuator, silicon photonics

PACS: 42.82.Et, 42.30.Lr, 42.82.Bq, 42.79.Sz **DOI:** 10.1088/1674-1056/27/12/124208

1. Introduction

The demand for data is rapidly increasing and, therefore, the further enhancement of information capacity has become a popular topic of research. Dense wavelength division multiplexing (DWDM) technology is a cost-effective solution to expand the capacity of optical interconnects, which offers high bandwidth utilization. Wavelength division multiplexer/demultiplexer is a key component in the DWDM system. Arrayed waveguide gratings (AWGs)[1–3] have been increasingly popular among all devices that can realize wavelength division multiplexing/demultiplexing applications. This is due to the fact that the AWG can realize the multiplexing/demultiplexing function with a large number of channels. The DWDM system requires large channel and small channel spacing, which needs to strictly control the wavelength drift of AWG. Consequently, new methods to realize the precise positioning of AWGs on the ITUT grid have become a necessity.

Silicon photonics,[4–6] which are compatible with the mature complementary metal–oxide semiconductor (CMOS) technology, are a promising solution for future high-speed optical interconnections because they possesses high refractive contrast and the silicon-on-insulator (SOI) based waveguides allow small bent radius, small footprint and, therefore, high level integration of many optical functions[7–14] on a single chip. However, the high refractive contrast of SOI can cause some issues, one of which is its sensitivity to dimensional variation. Take the arrayed waveguide grating (AWG) for instance. Because the AWG is a large device, it is more vulnerable to the kind of dimensional variation and small dimensional variation in its fabrication that will introduce a large peak wavelength shift. Consequently, the methods[15] to stabilize and tune or compensate for optical wavelength drift are of great interest.

In the DWDM system, the optical power of signals with different wavelengths cannot stay the same due to the non-uniformity of the lasers' output power, the different absorption losses of different signals in their transmission, and the intrinsic non-flat gains of erbium doped amplifier in different channels. The non-uniformities of optical signals with different wavelengths will badly influence the following optical transmission and processing. So methods[16–19] must be taken to ensure that the optical powers of different signals are balanced.

In this paper, a 16-channel SOI-based wavelength division multiplexer/demultiplexer with dual-tunable function is demonstrated, which can realize the wavelength division multiplexing/demultiplexing function, the peak-wavelength tuning function, and the optical power tuning function.

*Project supported by the National Key Research and Development Program of China (Grant No. 2016YFB0402504) and the National Nature Science Foundation of China (Grant No. 61435013).

†Corresponding author. E-mail: wy1022@semi.ac.cn
‡Corresponding author. E-mail: wuyuanda@semi.ac.cn

© 2018 Chinese Physical Society and IOP Publishing Ltd

2. Design and fabrication

2.1. Principle and structure

Figure 1 (a) is a schematic diagram of the 16-channel SOI-based wavelength division multiplexer/demultiplexer with dual-tunable function, which consists of a 16-channel AWG for wavelength division multiplexing/demultiplexing, a heater with a parallel structure for peak wavelength tuning and VOAs[16] based on p–i–n carrier-injection structure for optical power tuning. The detailed structures of the heater and the VOAs are shown in Figs. 1(b) and 1(c), respectively.

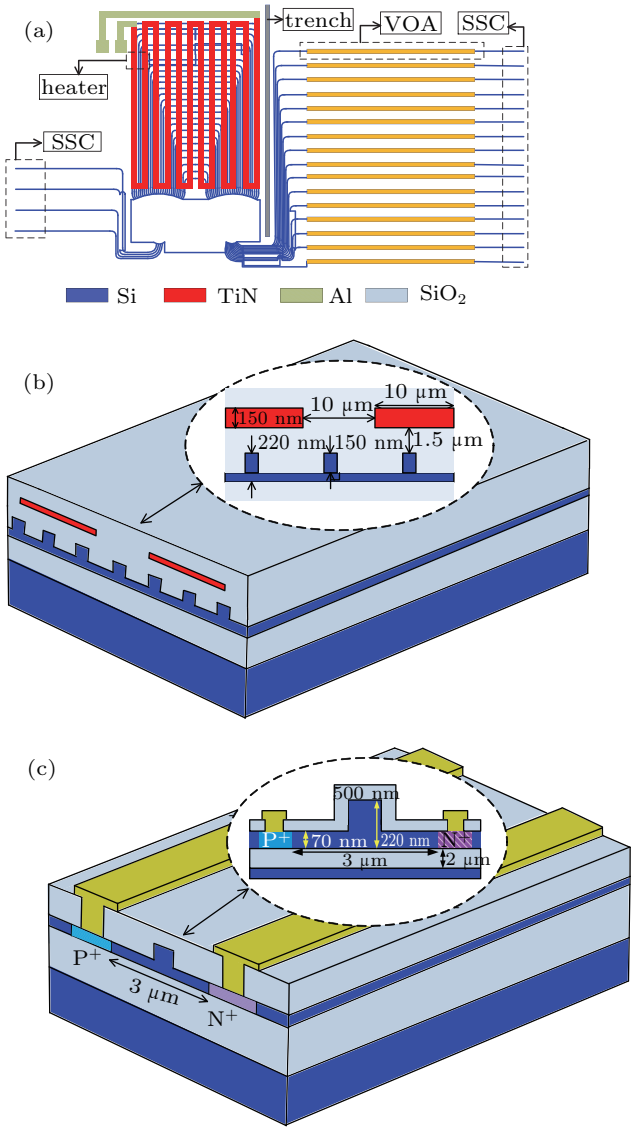


Fig. 1. (color online) Schematic diagram of (a) top view of wavelength division multiplexer/demultiplexer with dual-tunable function, (b) heater structure, and (c) VOA structure.

A typical AWG consists of input/output waveguides, input/output slab waveguides, and arrayed waveguides. According to the theory of multi-beam interference, light propagation in the AWG satisfies the grating diffraction equation, as follows:

$$n_{\mathrm{s}}(\lambda)\, d \sin\theta_{\mathrm{i}} + n_{\mathrm{s}}(\lambda)\, d \sin\theta_{\mathrm{o}} + n_{\mathrm{c}}(\lambda)\,\Delta L = m\lambda, \qquad (1)$$

where $n_{\mathrm{s}}/n_{\mathrm{c}}$ is the refractive index of the slab waveguide/arrayed waveguide; λ is the wavelength of optical signal; d is the minimum separation distance between the adjacent arrayed waveguides; $\theta_{\mathrm{i}}/\theta_{\mathrm{o}}$ is the diffraction angel at the input/output slab; ΔL is the length difference between the adjacent arrayed waveguides; m is the diffraction order.

From Eq. (1) it can be seen that if the fabricated dimension (refractive index) of the waveguide deviates from the designed value, the focused wavelength at a particular output waveguide will also change. The designed parameters of the AWG are shown in Table 1.

Table 1. Design parameters of silicon nanowire AWG.

Symbol	Quantity	Value
H	thickness of top silicon of SOI	220 nm
w	waveguide width	500 nm
n_{s}	effective refractive index of slab waveguide	2.849257
n_{c}	effective refractive index of arrayed waveguide	2.53455
n_{g}	the group index of arrayed waveguide	3.796747
λ	central wavelength	1.55252 μm
$\Delta\lambda$	channel spacing	1.6 nm
N_{i}	number of input channels	8
N_{o}	number of output channels	16
N	number of arrayed waveguides	77
FSR	free spectral range	25.9 nm
d	pitch width of arrayed waveguide	2.25 μm
D_{h}	heater spacing	10 μm
W_{h}	heater width	10 μm

The heater can be used to compensate for optical wavelength drift. According to the thermo–optic (TO) effect, the peak wavelength shift ($\Delta\lambda$) arising from the change of temperature (ΔT) can be calculated from Eqs. (2) and (3). The TO coefficient ($\mathrm{d}n/\mathrm{d}T$) of Si equals 1.84×10^{-4}/K, and that of SiO_2 equals 1.0×10^{-5}/K.

$$\Delta\lambda = \frac{\Delta n_{\mathrm{eff}}}{n_{\mathrm{g}}}\cdot\lambda_0, \qquad (2)$$

$$\Delta n_{\mathrm{eff}} = \frac{\partial n_{\mathrm{eff}}}{\partial n_{\mathrm{Si}}}\cdot\Delta n_{\mathrm{Si}} + \frac{\partial n_{\mathrm{eff}}}{\partial n_{\mathrm{SiO_2}}}\cdot\Delta n_{\mathrm{SiO_2}}, \qquad (3)$$

where $\Delta n_{\mathrm{Si}}/\Delta n_{\mathrm{SiO_2}}$ represents the change in refractive index of the Si/SiO_2 caused by the change of temperature, and therefore the effective index of the waveguide (n_{eff}) is also changed; n_{g} is the group index of the waveguide; λ_0 is the peak wavelength of a certain channel.

To tune the output optical power of each channel, according to the plasma dispersion effect of silicon, at 1550 nm the index change and the absorption coefficient change can be obtained from the well-known Soref empirical equations:

$$\Delta n = -\left[8.8\times10^{-22}\Delta N_{\mathrm{e}} + 8.5\times10^{-18}\left(\Delta N_{\mathrm{h}}\right)^{0.8}\right], \qquad (4)$$

$$\Delta\alpha = 8.5\times10^{-18}\Delta N_{\mathrm{e}} + 6.0\times10^{-18}\Delta N_{\mathrm{h}}, \qquad (5)$$

where ΔN_e and ΔN_h are the concentration of electrons and holes, respectively; Δn and $\Delta\alpha$, respectively represent the change of refractive index and absorption coefficient

Figure 1(c) shows the structure of a VOA based on SOI, which consists of a straight rib waveguide and a lateral p–i–n diode. When forward bias is applied to the Al electrodes, carriers will be injected into the intrinsic area, and then $\Delta\alpha$ of the intrinsic area will increase according to Eq. (5). When optical signal passes through the intrinsic zone, the optical power will be attenuated. The relationship between attenuation (Att.) and $\Delta\alpha$ is

$$\begin{aligned}\text{Att.} &= -10\log\left(\frac{P}{P_0}\right) = -10\log\left(\frac{P_0\,\mathrm{e}^{-\Delta\alpha L}}{P_0}\right)\\ &= 10\Delta\alpha\cdot\log(\mathrm{e})\cdot L,\end{aligned} \tag{6}$$

where P and P_0 are the optical power of output and input light respectively, and L is the modulation length.

As shown in Figs. 1(b) and 1(c), the thicknesses of top silicon and the buried oxide are 220 nm and 2 μm, respectively. The thickness of the slab is 70 nm, and the width of the waveguide is 500 nm to ensure the single mode propagation. The distance between the $P+$ region and the $N+$ region is 3 μm so that there is hardly any absorption loss caused by the doping position. To tune the peak wavelength of AWG, a 10-μm wide heater with a parallel structure is fabricated on the top of the AWG device and the heater spacing is 10 μm as shown in Figs. 1(a) and 1(b). The distance between the heater layer and the waveguide layer is 1.5 μm, so that there is no extra loss caused by the metal absorption. A deep trench for thermal insulation with VOAs is designed beside the heater as shown in Fig. 1(a).

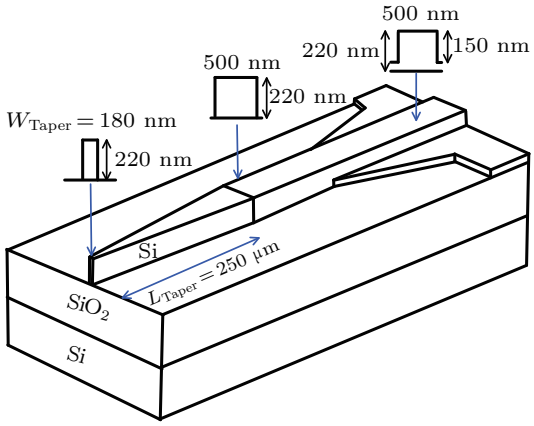


Fig. 2. Diagram of three-dimensional structure of SSC.

Spot size converters (SSCs) are used to reduce the coupling loss caused by the mode-size mismatch between the input/output fiber and the input/output waveguides of the wavelength division multiplexer, and the diagram of three-dimensional structure of the SSC is shown in Fig. 2. Considering the tolerance of fabrication process, the beginning width (W_{Taper}) and the length (L_{Taper}) of the taper are designed to be 180 nm and 250 μm, respectively

2.2. Fabrication

The wavelength division multiplexer/demultiplexer with dual-tunable function was fabricated as follows. First, the rib waveguides was fabricated by deep ultraviolet lithography (DUVL) process and inductively coupled plasma (ICP) etching process. Then, the $P+$ region and $N+$ region were formed by boron and phosphorus implantation, respectively, and then the chip was annealed at 1050 °C for 30 min to recrystallize the doping zone. Next, the Si slab was etched to fabricate the channel-type tapers for the SSCs in the input/output waveguide region. A 1.5-μm thick SiO_2 layer was then fabricated by plasma-enhanced chemical vapor deposition (PECVD) followed by the fabrication of 150-nm thick TiN as a heater. Finally, SiO_2 as the upper cladding layer was deposited by PECVD process and then 1-μm thick Al was deposited to generate the leadwire electrodes and the Al pads. The fabricated device is shown in Fig. 3, and the total size of the wavelength division multiplexer is 3 mm×1.2 mm.

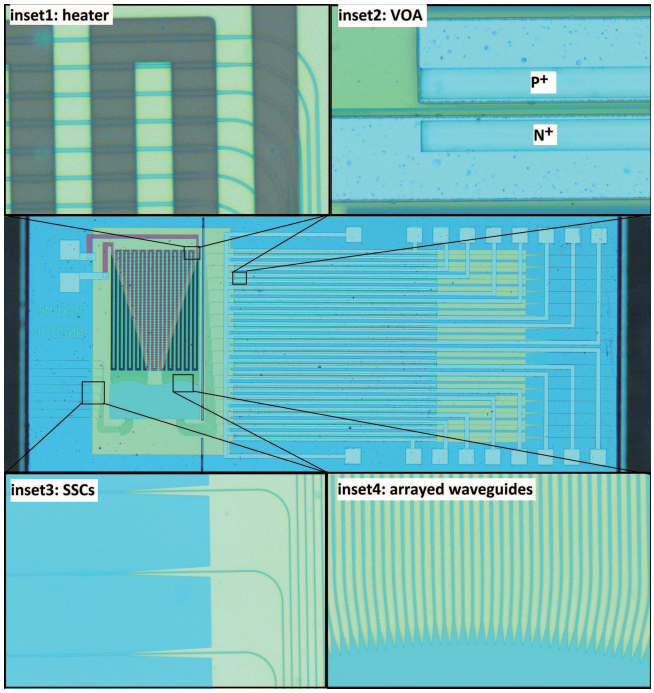


Fig. 3. (color online) Micrograph of fabricated wavelength division multiplexer.

3. Measurement and discussion

3.1. Peak wavelength tuning

First, the optical property of the AWG before (0 V) and after (60 V) heating were examined as shown in Fig. 4(a). From Fig. 4(a), it can be seen that the insertion loss on chip of the AWG is about 3.7 dB–5.7 dB and the crosstalk is about 7.5 dB–9 dB. The high crosstalk could result from the beam

defocusing at the output waveguides due to unequal phase shifts of arrayed waveguides. Some methods can be taken to further reduce the crosstalk. One is to optimize the fabrication process, and the other is to take some special structures such as a phase-error-compensating structure[20] to reduce the phase error caused by fabrication process; the boundary structures between the input/output slab waveguides and the arrayed waveguides can be further optimized to reduce the mutual coupling between two waveguides near the boundary, such as by taking parabolic tapers[2] or bi-level tapers.[3]

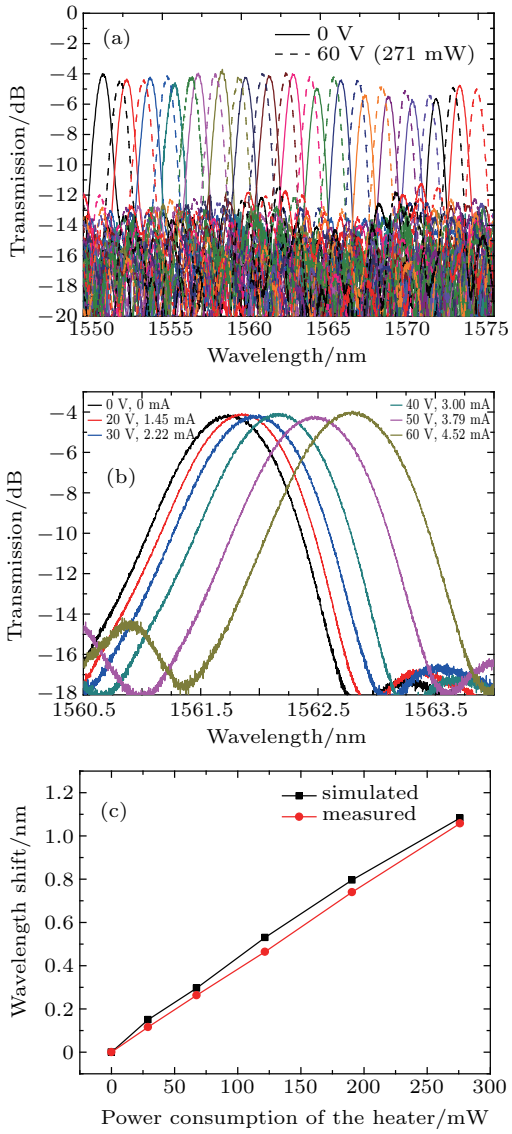


Fig. 4. (color online) (a) Transmission of the 8th channel under different voltage, (b) transmission of the 8th channel under different voltage, and(c) simulated and measured wavelength shift varying with power consumption of heater. of wavelength division multiplexer/demultiplexer.

Table 2. Tested results about peak wavelength tunability of the 8th channel.

Applied voltage/V	Injected current/mA	Peak wavelength/nm	Wavelength tunability/nm	Modulation efficiency/(nm/W)
		1561.733	0	
20	1.45	1561.849	0.116	
30	2.22	1561.996	0.263	3.9244
40	3	1562.197	0.464	
50	3.79	1562.473	0.74	
60	4.52	1562.791	1.058	

3.2. Output optical power tuning

The results of the test of the tunability of the output optical power are shown in Fig. 5, which is a normalized transmission spectrum of the wavelength division multiplexer/demultiplexer with voltages applied on the VOAs. The 16 channels are equally divided into four groups. Different levels of attenuation (att.) are achieved in different groups (0, 5, 10, 15 dB respectively for each group) and the 4 channels in the same group are driven to realize the equivalent attenuation.

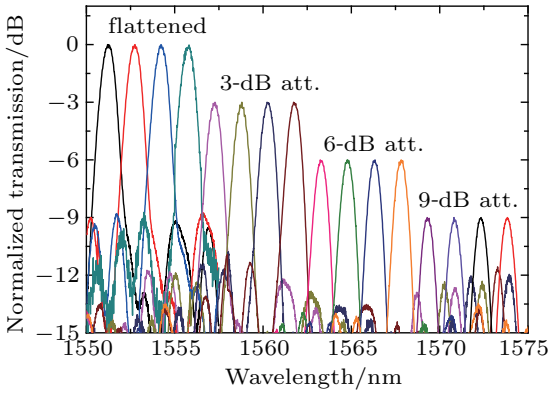


Fig. 5. (color online) Plots of normalized transmission versus wavelength of wavelength division multiplexer/demultiplexer.

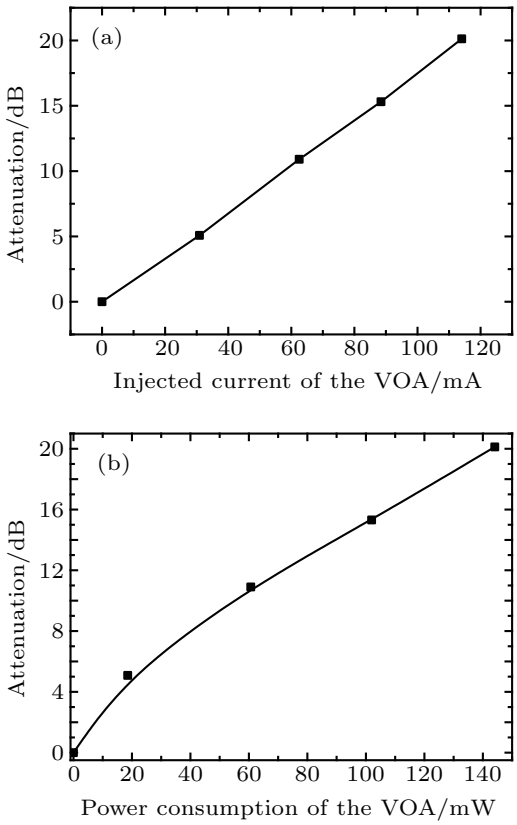


Fig. 6. Performance of the optical power tuning units, showing dependence of attenuation on (a) injected current and (b) power consumption.

The performance of the optical power tuning units is then tested, as shown in Figs. 6 and 7. Figures 6(a) and 6(b) show the dependence of the attenuation on injected current and power consumption, respectively. From Fig. 6(a) it can be seen that the attenuation rises linearly as injected current increases. The injected current is 114.05 mA at 20-dB attenuation and it can be obtained from Fig. 6(b) that the power consumption at 20-dB attenuation is 144.07 mW. The corresponding results are listed in Table 3. Figure 7 shows the response of optical power tuning units with a 2-MHz injection pulse. In a 0 V–2 V bias operation, the rising time and falling time of the optical power tuning units are 35 ns and 42 ns, respectively.

Table 3. The optical power tuning of the wavelength division multiplexer/demultiplexer.

Applied voltage/V	Injected current/mA	Attenuation/dB	Attenuation efficiency/(dB/mA)
0.60	30.89	5.08	0.164
0.97	62.52	10.9	0.174
1.15	88.45	15.31	0.173
1.26	114.05	20.12	0.176

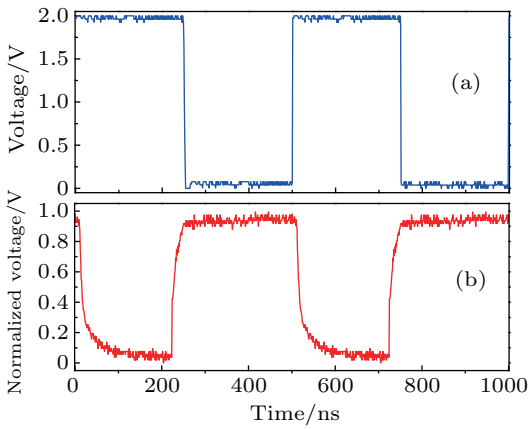


Fig. 7. (color online) (a) 2-MHz square electrical signal applied to optical power tuning units; (b) measured dynamic response of optical power tuning units.

4. Comparisons and creation

In previous work, wavelength tunable AWG based on the SOI[15] has been reported only once, which was fabricated by Nanyang technological university, but its heater structure and fabrication process are relatively complex, including the deposition of five kinds of metal materials, chemical–mechanical polishing process, physical vapor deposition and electrochemical-plating. In the present work, the fabrication process is simplified, which involves the deposition of two kinds of metal materials and metal liftoff process. The modulation efficiency of the device in this work is 3.9 nm/mW, which is in agreement with that in Ref. [15].

Some optical power tunable AWGs have been reported, such as an AWG with VOAs based on SOI with a several-micron top silicon layer,[21] a variable multiplexer/demultiplexer based on silica,[22] and a silica-based AWG with a silicon-nanowire VOA array.[16] However, the silicon-nanowire AWG monolithically integrated with electro-absorption VOA based on SOI with a sub-micron top silicon layer has rarely been reported. Comparisons of the modulation efficiency between our AWG and the typical AWG reported by Nishi *et al.*[16] are made, which is a silica-based AWG hetero-integrated with a silicon-nanowire VOA array. The power consumption of the device in Ref. [16] is 45.8 mW at 20-dB attenuation, while the power consumption of the device in the present work is 144.07 mW at 20-dB attenuation, which seems to be not satisfactory. However, the modulation length of the VOA in Ref. [16] is 5 mm while ours is 1 mm, and it has been reported that longer modulation length results in smaller power consumption,[23] so the power consumption of our device may be cut down by increasing the modulation length.

Although the wavelength tunable AWG and optical power tuning AWG have been reported, the dual-tuning AWGs with both wavelength tuning and optical power tuning based on SOI have not yet been reported. In this work, we have proposed a dual-tuning AWG with wavelength tuning structure and optical power tuning structure, which can solve the problem of wavelength shift and unbalanced output power of AWG simultaneously.

5. Conclusions and perspectives

A 16-channel SOI-based wavelength division multiplexer/demultiplexer, which is both output optical power tunable and peak wavelength tunable, is demonstrated. The wavelength division multiplexer/demultiplexer consists of an arrayed waveguide grating for wavelength division multiplxing/demultiplexing, a VOA based on p–i–n carrier-injection structure for optical power tuning and a heater for peak wavelength tuning. The experimental results show that the insertion loss of the device is 3.7 dB–5.7 dB, the crosstalk is 7.5 dB–9 dB. The methods must be taken to reduce the crosstalk, such as further optimizing the structure between the input/output slab waveguides and the arrayed waveguides. For the tunability of the peak wavelength, 1.058-nm wavelength shift is achieved with 271.2-mW power consumption, and the modulation efficiency is 3.9244 nm/W. For the tunability of the output optical power, the optical power-level control is achieved in all 16 channels and 20-dB attenuation is achieved with power consumption of 144.07 mW. The power consumption can be cut down by appropriately increasing the modulation length of the optical power tuning units or adopting a series structure. The response of the VOA is tested and the rising and falling time of VOA are 35 ns and 42 ns, respectively.

References

[1] Li K L, An J M, Zhang J S, Wang Y, Wang L L, Li J G, Wu Y D, Yin X J and Hu X W 2016 *Chin. Phys. B* **25** 124209

[2] Ye T, Fu Y, Qiao L and Chu T 2014 *Opt. Express* **22** 31899

[3] Park J, Joo J, Park H, Kwack M J and Kim G 2015 *Silicon photonics X* February 7–12, 2015, California, USA, p. 936705

[4] Feilchenfeld N B, Nummy K, Barwicz T, Gill D, Kiewra E, Leidy R, Orcutt J S, Rosenberg J, Stricker A D, Whiting C, Ayala J, Cucci B, Dang D, Doan T, Ghosal M, Khater M, McLean K, Porth B, Sowinski Z, Willets C, Xiong C, Yu C, Yum S, Giewont K and Green W M J 2017 *Advanced etch technology for nanopatterning VI*, February 26–March 2, 2017, California, SUA, p. 101490D

[5] Chiles J and Fathpour S 2017 *J. Opt.* **19** 053001

[6] Li X Y, Yu Y D and Yu J Z 2013 *Physics* **42** 272 (in Chinese)

[7] Ren B, Hou Y and Liang Y 2016 *J. Semicond.* **37** 124001

[8] Spott A, Peters J, Davenport M L, Stanton E J, Merritt C D, Bewl W W, Vurgaftman I, Kim C S, Meyer J R, Kirch J, Mawst L J, Botez D and Bowers J E 2016 *Optica* **3** 545

[9] Wu W, Cheng B, Zheng J, Liu Z, Li C, Zuo Y and Xue C 2017 *J. Semicond.* **38** 114003

[10] Wang Z, Gao Y L, Kashi A S, Cartledge J C and Knights A P 2016 *J. Lightwave Technol.* **34** 3675

[11] Song B, Stagarescu C, Ristic S, Behfar A and Klamkin J 2016 *Opt. Express* **24** 10435

[12] Zhao Z, Liu J, Liu Y and Zhu N 2017 *J. Semicond.* **18** 121001

[13] Shin M J, Ban Y, Yu B M, Rhim J, Zimmermann L and Choi W Y 2016 *IEEE J. Sel. Top. Quantum Electron.* **22** 3400207

[14] Zhao Y, Jia H, Ding J, Zhang L, Fu X and Yang L 2016 *J. Semicond.* **37** 114008

[15] Yang Y, Hu X, Song J, Fang Q, Yu M and Tu X 2015 *IEEE Photon. Technol. Lett.* **27** 2351

[16] Nishi H, Tsuchizawa T, Watanabe T, Shinojima H, Park S, Kou R, Yamada K and Itabashi S I 2010 *Appl. Phys. Express* **3** 102203

[17] Day I, Whiteman R, House A A, Knights A P, Drake J and Asghari M 2002 *Integrated Photonics Research*, July 17–19, 2002, Vancouver, Canada, p. IFA5

[18] Zheng D W, Fong J, Liang H, Kung C C, Qian W and Smith B T 2006 *Optical Fiber Communication Conference and* 2006 *National Fiber Optic Engineers Conference*, March 5–10, 2006, CA, USA, p. 1960

[19] Ren M Z, Zhang J S, An J M, Wang Y, Wang L L, Li J G, Wu Y D, Yin X J and Hu X W 2017 *Chin. Phys. B* **26** 074221

[20] Gehl M, Trotter D, Starbuck A, Pomerene A, Lentine A L and DeRose C 2017 *Opt. Express* **25** 6320

[21] Fang Q, Song J, Zhang G, Yu M, Liu Y, Lo G Q and Kwong D L 2009 *IEEE Photon. Technol. Lett.* **21** 319

[22] Itoh M, Watanabe K, Nasu Y and Yamazaki H 2007 33*rd European conference and exhibition of optical communication*, September 16–20, 2007, Berlin, Germany, p. 2.5.1

[23] Yuan P, Wang Y, Wu Y, An J and Hu X 2018 *Opt. Laser Technol.* **102** 166